Nonlinear effects of beam-plasma instabilities on neutralized propagation of intense ion beams in background plasma

Edward A. Startsev,[a], Igor Kaganovich, and Ronald C. Davidson

Princeton Plasma Physics Laboratory, Princeton NJ, USA

Abstract. The streaming of the ion beam relative to the background plasma can cause the development of fast electrostatic collective instabilities. In this paper we examine numerically the defocusing effects of two-stream instability on the ion beam propagating in the neutralizing plasma. The scaling laws of the average de-focusing forces on the beam ions are identified, and confirmed by comparison with numerical simulations. These scalings can be used in the development of realistic ion beam compression scenarios in present and next-generation ion-beam-driven experiments.

1 Introduction

To achieve energy densities necessary for ion-beam-driven high energy density physics and heavy ion fusion applications, the intense ion beam pulse must be compressed transversely and longitudinally before it reaches the target. To achieve maximum compression, the intense ion beam pulse must propagate through background plasma which can neutralize the beam space-charge and provide a significant neutralization of the beam current leading to almost ballistic focusing of the intense ion beam with radius r_b much larger than collisionless plasma skin depth λ_p. For a thin and infinitely heavy ion beam with $r_b \lesssim \lambda_p$ the beam current density is only partially neutralized, so that remaining current density produces azimuthal magnetic field that pinches the beam [1]. On the other hand the streaming of the moderately heavy ion beam relative to background plasma can cause the development of fast electrostatic collective instabilities between beam ions and background electrons. As it's demonstrated numerically in this paper using particle-in-cell code LSP [2], the nonlinear stage of these instabilities produces fluctuating electrostatic fields which cause significant drag on background plasma electrons and result in producing local current densities which may significantly exceed the beam current density [3]. These overneutralizing background electron current densities reverse the beam magnetic field and lead to the beam transverse defocusing. At the same time, the ponderomotive force of the unstable wave pushes background electrons transversely away from the unstable region inside the beam, which creates the ambipolar electric field, which also leads to the ion beam transverse defocusing.

2 Numerical simulations of ion beam propagation in neutralizing plasma

To benchmark scaling laws for these nonlinear defocusing forces we simulated propagation of hydrogen and lithium ion beams of different duration and densities in the background plasma of different densities. The hydrogen beam simulations were carried out for the following parameters: the ion beam has Gaussian density profile and pulse duration $T = 12ns$, with

[a] e-mail: estarts@pppl.gov.Research supported by the U.S. Department of Energy.

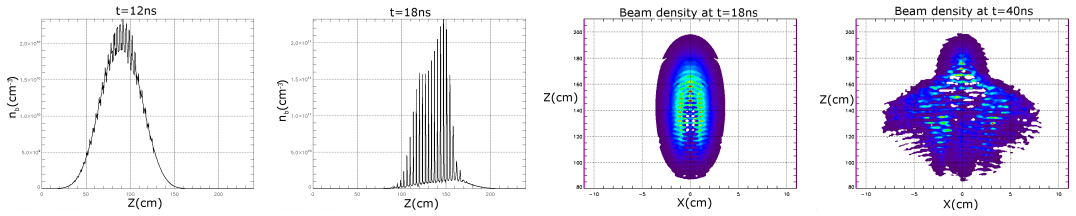

Fig. 1. Longitudinal beam density profile at $t = 12ns$ (a) and $t = 18ns$ (b) and color plots of beam density at $t = 18ns$ (c) and $t = 40ns$ (d)

beam velocity $v_b = c/2$, where c is the speed of light in vacuo; the beam density is $n_b = 2 \times 10^{10} cm^{-3}$, and the beam radius is $r_b = 2cm$; the beam propagates through a stationary, singly-ionized carbon plasma with plasma density $n_p = 2 \times 10^{11} cm^{-3}$. The results of the simulations are illustrated in Fig. 1. At time $t = 0$ the ion beam enters the plasma at $Z = 0$. As shown in Fig.1(a) , at time $t = 12ns$ the two-stream instability between the beam ions and the plasma electrons begins to develop and is completely developed to the saturation level by time $t = 18ns$ [Fig. 1(a)]. At this time the hydrogen ion beam density is modulated with density variations of order 100% of the original beam density. Figure 2 shows the longitudinal phase space of the beam ions(red) and plasma electrons(blue) at $t = 18ns$. Note that at the time of saturation at $t = 18ns$, the beam ions begin to be trapped by the nonlinear wave while background electrons are completely trapped by the wave and perform nonlinear oscillations with amplitude $v_m^e \sim v_b$. Figure 3 shows the azimuthal magnetic field and the

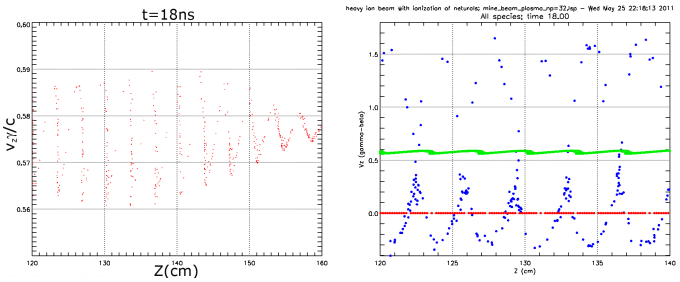

Fig. 2. Beam (red) (a) and background electrons (blue) (b) phase-space $z - v_z\gamma$ at $t = 18ns$.

longitudinal current density. As shown in Fig. 3(a,b), at $t = 12ns$ the beam current density is partially neutralized by the return current of the background plasma electrons. The resulting net current density produces magnetic field that results in a focusing force which leads to the beam pinching. But as the instability develops and saturates at $t = 18ns$, the longitudinal current density and magnetic field change sign [Fig. 3(c,d)]. The resulting reversed magnetic field associated with a net current density leads to a defocusing of the ion beam pulse. The average radial component of the electric field (averaged over the fluctuations) at the time when the instability saturates at $t = 18ns$ is shown in Fig. 4. The large average electric field has an ambipolar structure and also contributes to the ion beam defocusing. Figs. 1(c,d) show the ion beam density at two instants of time, $t = 18ns$ and $t = 40ns$. Note that after $40ns$ the part of the beam where the instability has significantly developed is completely defocused, while the beam head remains relatively unchanged.

Similar simulations have also been carried out for parameters relevant to the upcoming NDCX-II experiments[4] and the results are illustrated in Figs. 5 and 6. In these simulations a singly-ionized lithium ion beam with velocity $v_b = c/30$ propagates through a neutralizing singly ionized background carbon plasma with density $n_p = 0.55 \times 10^{11} cm^{-3}$. At the entrance into the plasma the beam density is $n_b = 2 \times 10^9 cm^{-3}$, the beam radius is $r_b = 1.41cm$ and

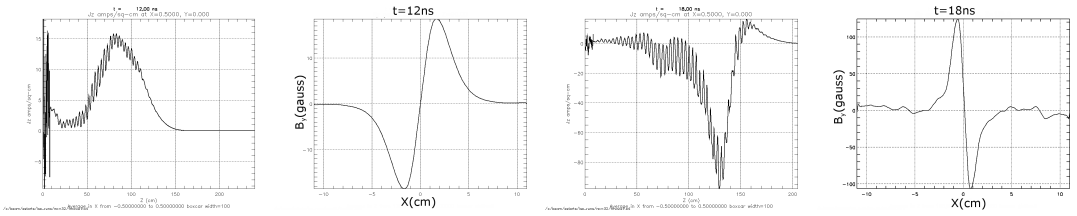

Fig. 3. Current density profile at $r = 0$ (a,c) and the transverse profile of associated azimuthal magnetic field in the middle of the beam (b,d) at $t = 12ns$ (a,b) and $t = 18ns$ (c,d).

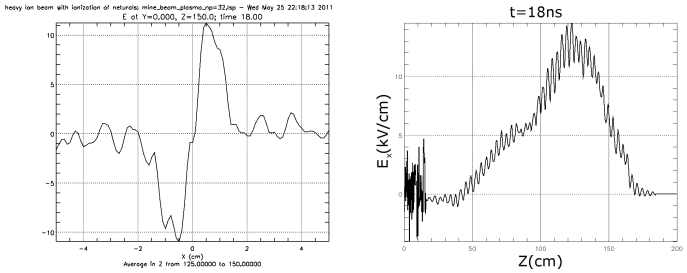

Fig. 4. Average radial electric field profiles, (a) transverse at the middle of the beam and (b) longitudinal at $r = 0$.

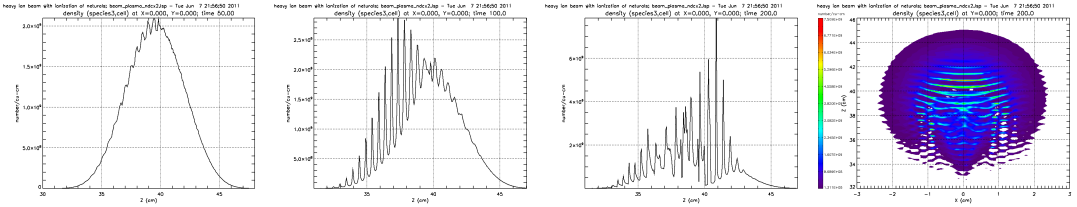

Fig. 5. Beam longitudinal density profile at $r = 0$ at $t = 50ns$ (a), $t = 100ns$ (b), $t = 200ns$ (c) and color plot of beam density at $t = 200ns$ (d).

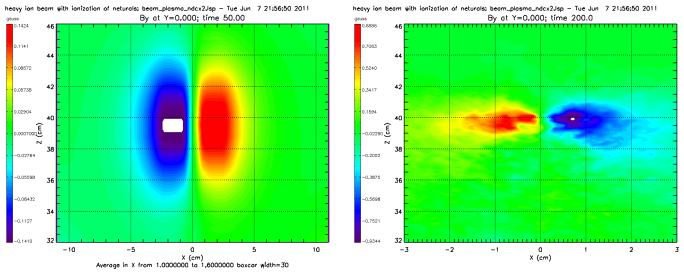

Fig. 6. Color plots of azimuthal magnetic field at $t = 50ns$ (a) and $t = 200ns$ (b).

the beam pulse duration is $T = 20ns$. After two meters of propagation at $t = 200ns$ the same two-stream instability is observed to develop and saturate, which results in longitudinal beam density variations of order 90 The unstable electric field fluctuations reverse the magnetic field [Fig. 6], but nonlinearly generated defocusing fields did not have enough time to significantly defocus the beam [Fig.5(d)]

3 Discussion and analytical estimates

In this section we make simple estimates of nolinearly generated transverse defocusing fields based on the physical picture observed in the simulations. The electrostatic field of the unstable wave produces an average longitudinal electron current density

$$< J_z^e >= -e < \delta n^e \delta v_z^e >= -e\frac{n_p}{v_b} < (\delta v_z^e)^2 >= -\frac{1}{2}\frac{n_p}{n_b}\left(\frac{v_m^e}{v_b}\right)^2 J_b. \quad (1)$$

This current density is reduced by the longitudinal inductive electric field by the factor $1/(1+r_b^2\omega_p^2/c^2)$. The total enhanced return current density reverses magnetic field to a value

$$< B_y >= \frac{4\pi}{c} < J_z > r_b \sim -\frac{2\pi e n_p r_b \beta_b}{(1+r_b^2\omega_p^2/c^2)}\left(\frac{v_m^e}{v_b}\right)^2. \quad (2)$$

The ponderomotive pressure of the unstable wave pushes electrons away from the unstable region inside the beam which sets up an ambipolar transverse electric field

$$e < E_x > \sim m_e\frac{(v_m^e)^2}{r_b}. \quad (3)$$

The transverse force on the beam ions due to electric field is $F_E = e < E_x >$, while the force due to magnetic field of the instability enhanced return current is

$$F_B = -e\frac{v_b}{c} < B_y > \sim \frac{F_E}{[1+c^2/(r_b^2\omega_p^2)]}. \quad (4)$$

For a beam with a radius $r_b\omega_p/c < 1$ the defocusing force is mainly due to ponderomotive pressure of the unstable wave on electrons, while for beams with $r_b\omega_p/c > 1$ both forces are of the same order. For arbitrary value of $r_b\omega_p/c$ the total defocusing force acting on the beam scales as

$$F \sim m_e\frac{v_b^2}{r_b}\left(\frac{v_m^e}{v_b}\right)^2 = m_e\frac{(v_m^e)^2}{r_b} = -\frac{dT_{eff}^e}{dr}, \quad (5)$$

where $T_{eff}^e = m_e(v_m^e)^2$ is the effective background electron osculation energy inside the ion beam and v_m^e/v_b can be estimated from particle trapping arguments as

$$\left(\frac{v_m^e}{v_b}\right) \sim min\left[\left(\frac{n_b}{n_p}\right)^{2/3}\left(\frac{m_b}{m_e}\right)^{1/3}; 1\right]. \quad (6)$$

The first limit corresponds to the instability saturated by the beam ion trapping, and the second is the saturation due to trapping of plasma electrons.

Knowing the defocusing forces on the ion beam, we can estimate the defocusing time T defined as time it takes the beam radius to double after the instability has developed and saturated, i.e, $\Delta r_b/r_b = 1$ and defocusing propagation distance $L = v_bT$

$$T \sim \left(\frac{r_b}{v_b}\right)\frac{(m_b/m_e)^{1/2}}{v_m^e/v_b}, \quad L \sim r_b\frac{(m_b/m_e)^{1/2}}{v_m^e/v_b}. \quad (7)$$

For the large beam densities, $n_b/n_p > (m_e/m_b)^{1/2}$, when $v_m/v_b \sim 1$ and instability is saturated by background electrons trapping, the defocusing time and distance are

$$T \sim \left(\frac{r_b}{v_b}\right)\left(\frac{m_b}{m_e}\right)^{1/2}, \quad L \sim r_b\left(\frac{m_b}{m_e}\right)^{1/2}. \quad (8)$$

For low density beams with $n_b/n_p < (m_e/m_b)^{1/2}$, the saturation is by the beam ions trapping, and the defocusing time and distance are

$$T \sim \left(\frac{r_b}{v_b}\right)\left(\frac{n_p}{n_b}\right)^{2/3}\left(\frac{m_b}{m_e}\right)^{1/6}, \quad L \sim r_b\left(\frac{n_p}{n_b}\right)^{2/3}\left(\frac{m_b}{m_e}\right)^{1/6}. \tag{9}$$

For the simulations of ion beam propagation in the plasma with parameters given in Sec. 2, the defocusing time is $T \sim 6ns$ and $T \sim 160ns$ for a proton beam and a lithium beam respectively, which is in qualitative agreement with the simulations. Note that total defocusing time observed in simulations also includes the time for instability to grow and saturate.

References

1. I. D. Kaganovich, G. Shvets, E. A. Startsev and R. C. Davidson, Phys. Plasmas **8**, (2001) 4180.
2. Need good LSP Reference, Nuclear Instruments and Methods in Physics Research **A577**, (2007) 79.
3. R. N. Sudan, Phys. Rev. Let. **37**, (1976) 1613.
4. Need Good NDCX-II refernce, Nuclear Instruments and Methods in Physics Research **A606**, (2009) 42.